Neuron

Supplemental Information

Targeted Ablation, Silencing, and Activation Establish Glycinergic Dorsal Horn Neurons as Key Components of a Spinal Gate for Pain and Itch

Edmund Foster, Hendrik Wildner, Laetitia Tudeau, Sabine Haueter, William T. Ralvenius, Monika Jegen, Helge Johannssen, Ladina Hösli, Karen Haenraets, Alexander Ghanem, Karl-Klaus Conzelmann, Michael Bösl, Hanns Ulrich Zeilhofer

Supplemental Data

Supplemental Figures

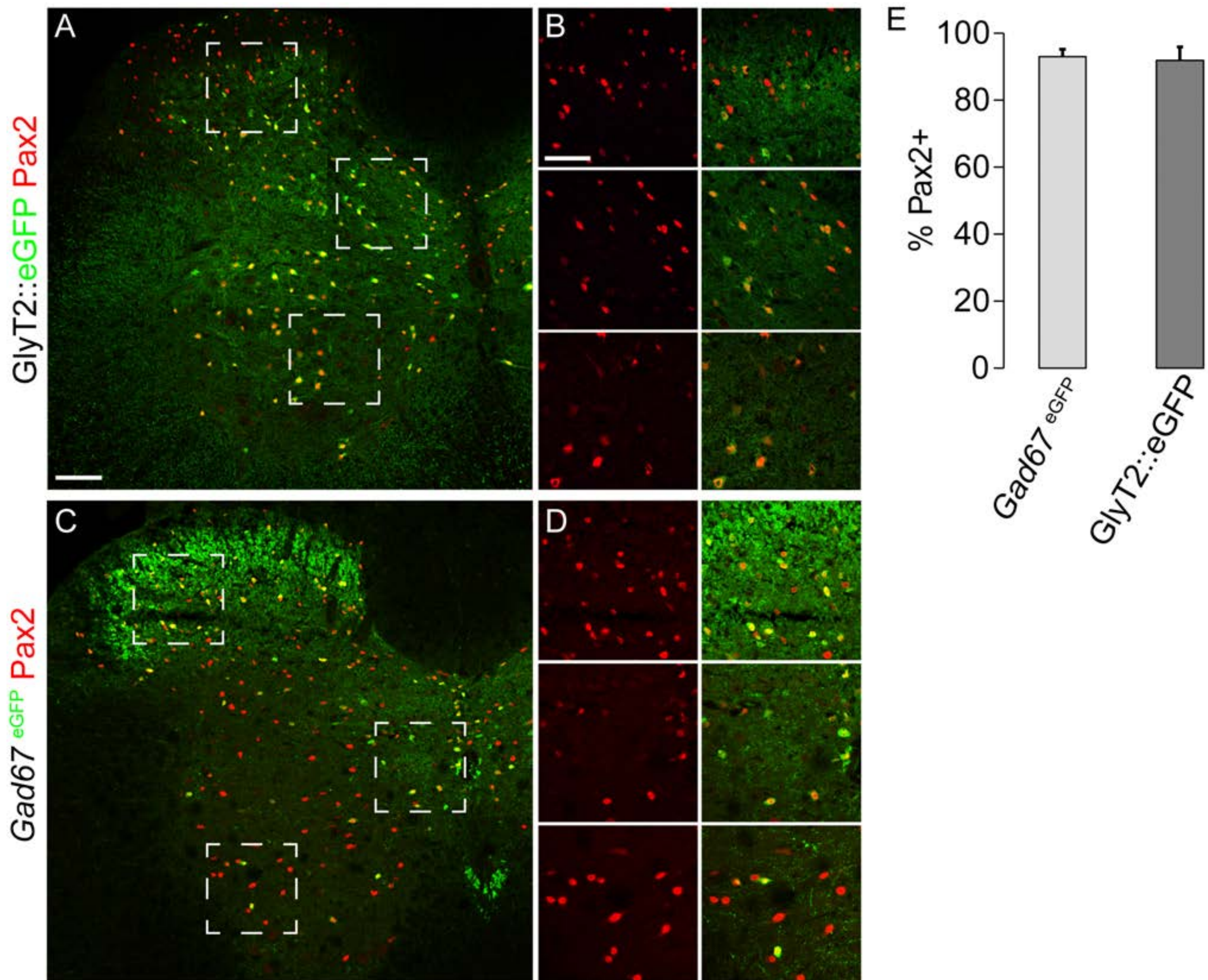

Figure S1 (related to Figure 1). Pax2 expression is maintained in inhibitory interneurons of the mouse spinal cord into adulthood

(A - D) At P60, Pax2 (red) expression is detectable in nearly all eGFP+ cells of GlyT2::eGFP and *Gad67*^{eGFP} transgenic mice. Magnifications in B and D correspond to the indicated areas in A and C, respectively. (E) Quantification of the number of eGFP+ neurons in *Gad67*^{eGFP} and GlyT2::eGFP transgenic mice also expressing Pax2. Mean ± SD. Scale bars: (A) 100 µm (B) 50 µm.

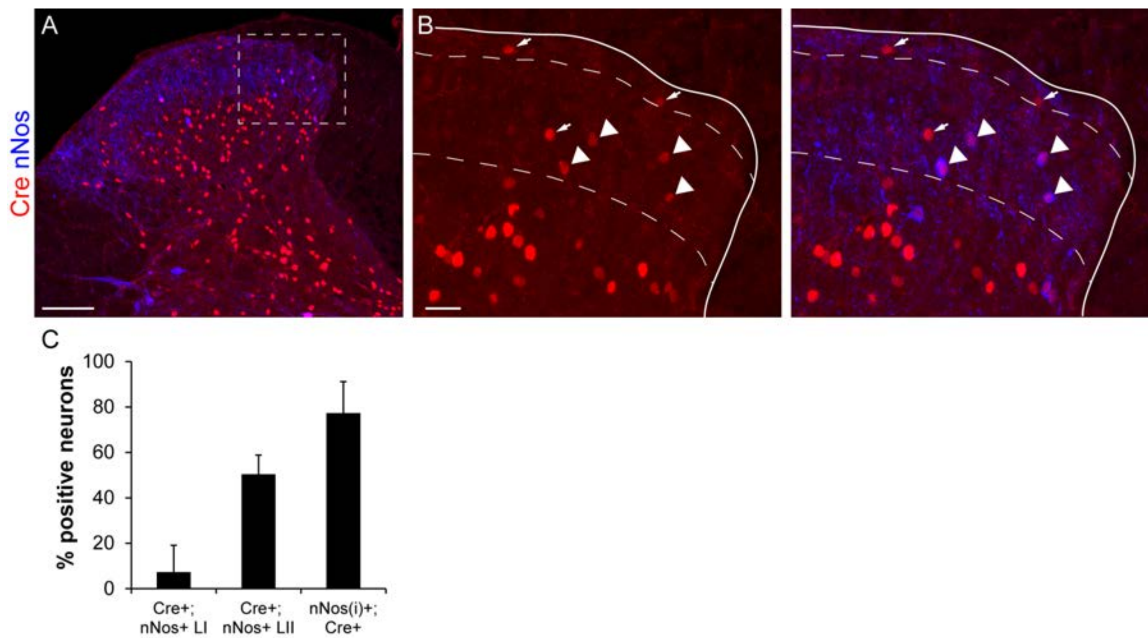

Figure S2 (related to Figure 1). nNos coexpression in superficial dorsal horn GlyT2::Cre+ neurons. (A) Spinal dorsal horn section of a GlyT2::Cre transgenic mouse stained against Cre and nNos proteins. Sections were co-stained for Pax2 to restrict analyses to inhibitory dorsal horn neuron. (B) Higher magnification. Arrowheads indicate double labeled neurons. Arrows indicate Cre+ / nNos- neurons. (C) Percentage of Cre+ neurons expressing nNos in laminae I (Cre+;nNos+ LI) and laminae II (Cre+;nNos+ LII) were determined as well as the percentage of inhibitory nNos neurons expressing Cre (nNos(i)+; Cre). To restrict the quantitative analysis to inhibitory nNos (nNos(i)+) dorsal horn neurons sections were co-stained for Pax2. Mean ± SD (n = 9 section from 3 mice). Scale bars, (A) 100 µm (B) 20 µm.

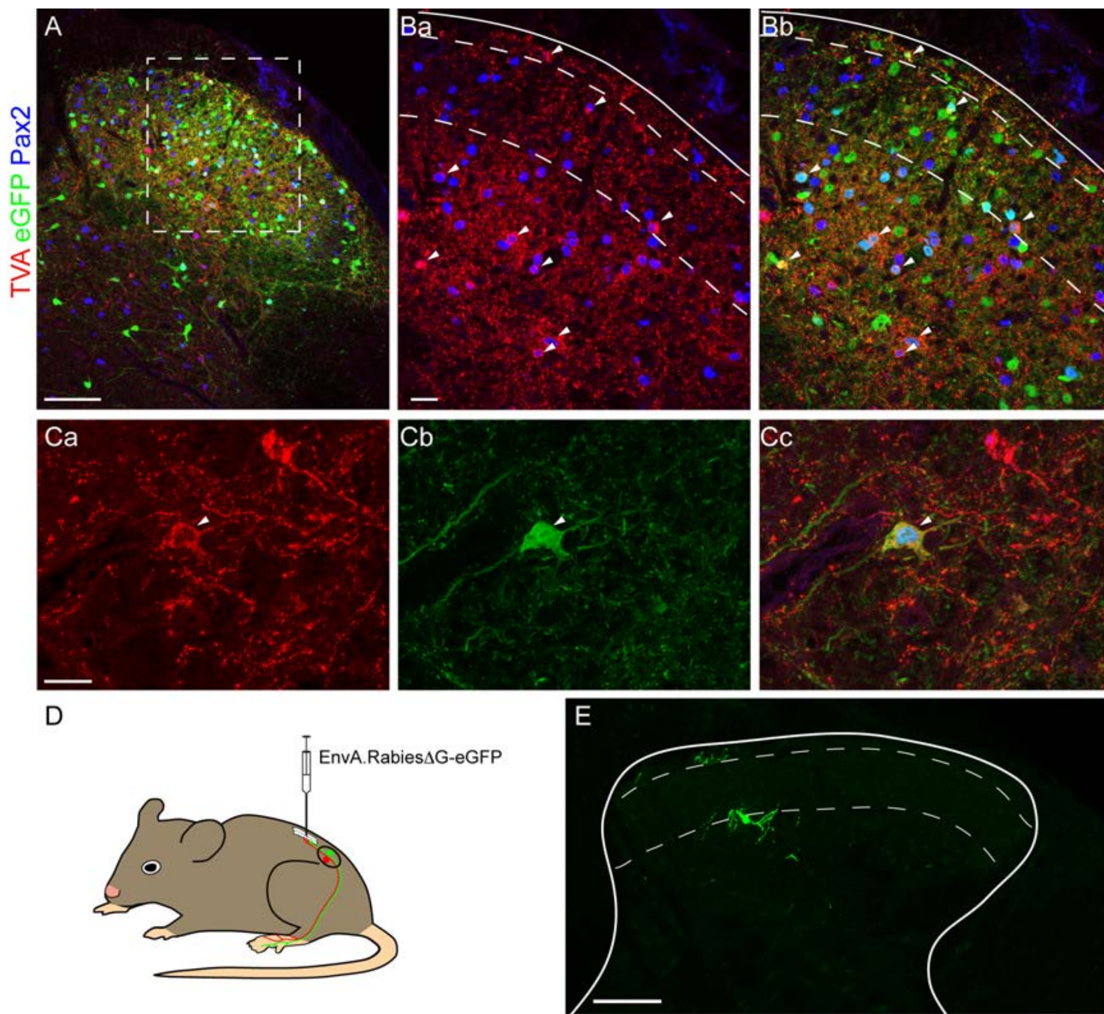

Figure S3 (related to Figure 2). Rabies virus-infected neurons 7 days after rabies virus injection into the spinal dorsal horn. (A - C) Spinal cord of GlyT2::Cre mice injected first with AAV.flex.TVA-2A-RabG and then with EnvA.RabiesΔG-eGFP. (A) Representative section of an injected spinal cord labeled with antibodies against TVA (red), eGFP (green) and Pax2 (blue). (Ba,b) Higher resolution picture demonstrating the presence of multiple primary infected cells (arrowheads, triple labeled cells). (Ca-c) Example of a neuron expressing TVA, GFP and Pax2. On average, 30 - 40 triple labeled cells were identified per section. From serial sections, we estimate that primary EnvA.RabiesΔG-eGFP infection occurred in about 2500 cells / spinal cord (n = 8 mice). (D, E) When EnvA.RabiesΔG-eGFP was injected into non-preinfected (TVA-negative) GlyT2::Cre mice, eGFP+ neurons occurred occasionally (0 - 7 cells / spinal cord, n = 4 mice), most likely due to very small contaminations of the EnvA.RabiesΔG-eGFP virus stock with non-pseudotyped virus. Scale bars, 100 µm (A, E), 20 µm (B, C).

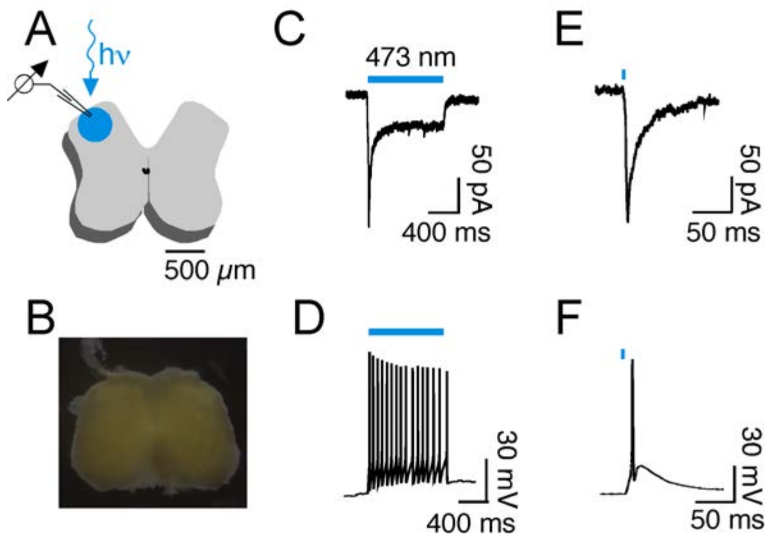

Figure S4 (related to Figure 4) Optogenetic characterization of inhibitory dorsal horn neurons. (A) Photocurrents and light-evoked action potentials in neurons recorded from slices obtained from vGAT::ChR2-eYFP BAC transgenic mice. (A) Blue light of 473 ± 5 nm wavelength was applied to one entire dorsal horn. (B) Distribution of the ChR2-eYFP fluorescence in a horizontal lumbar spinal cord slice. (C) Partially desensitizing photocurrent recorded from a lamina II neuron evoked by 1 s light exposure. (D) The same light stimulus evoked a train of action potentials in the current clamp mode, which is typical of inhibitory neurons in the superficial mouse spinal dorsal horn (Punnakkal et al., 2014). (E) Short photocurrent evoked by a 4 ms light stimulation. (F) Single action potential evoked by a 4 ms light stimulus.

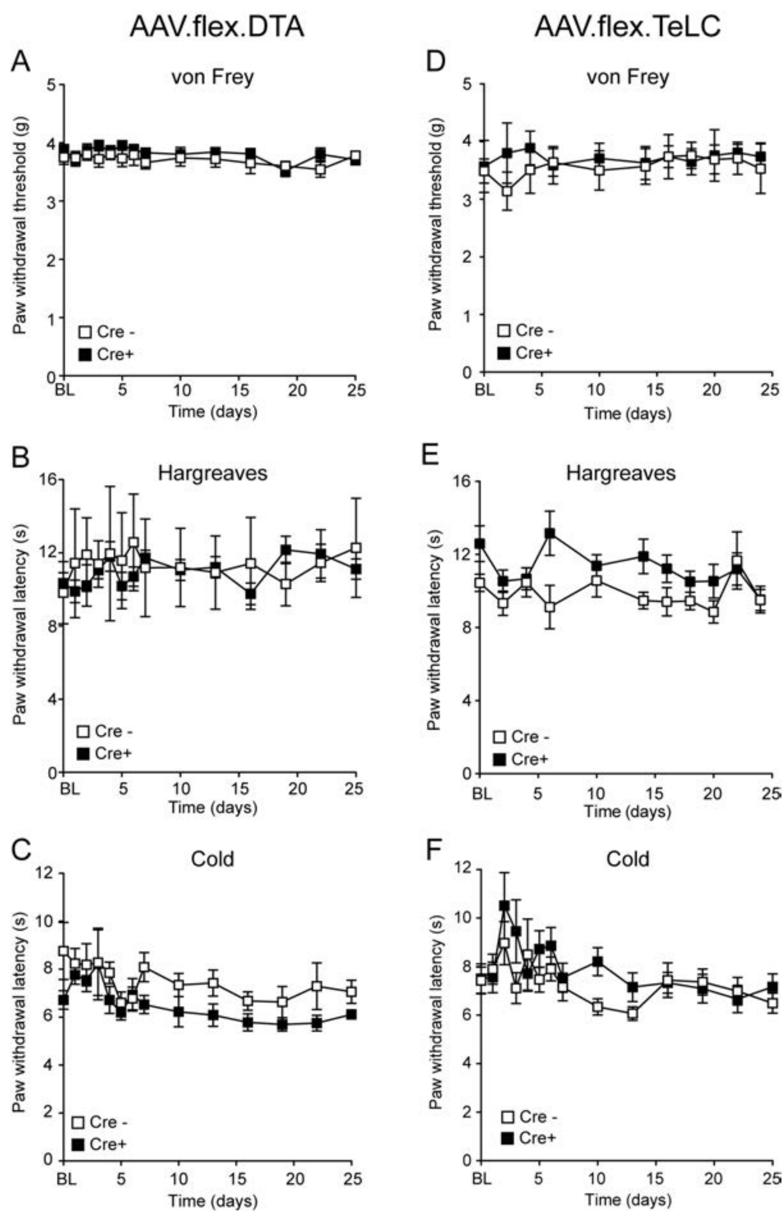

Figure S5 (related to Figures 5 and 7). Contralateral mechanical and thermal responses following contralateral ablation or silencing of spinal glycinergic neurons.
(A - C) Mechanical (A), heat (B), and noxious cold (C) sensitivities for the contralateral paw remained virtually unchanged after AAV.flex.DTA injection. Repeated measures ANOVA did not reveal significant genotype x time interactions between GlyT2::Cre+ and GlyT2::Cre- mice (von Frey: $F(13,221) = 0.57$, $P = 0.87$; Hargreaves: $F(13,221) = 1.06$, $P = 0.39$; cold: $F(13,143) = 0.44$, $P = 0.96$). (D - F) No mechanical and thermal sensitization developed after AAV.flex.TeLC injection. Repeated measures ANOVA: von Frey: $F(10,140) = 1.12$, $P = 0.35$; Hargreaves: $F(10,140) = 1.38$, $P = 0.20$; cold: $F(13,247) = 0.97$, $P = 0.48$). All error bars are SEM.

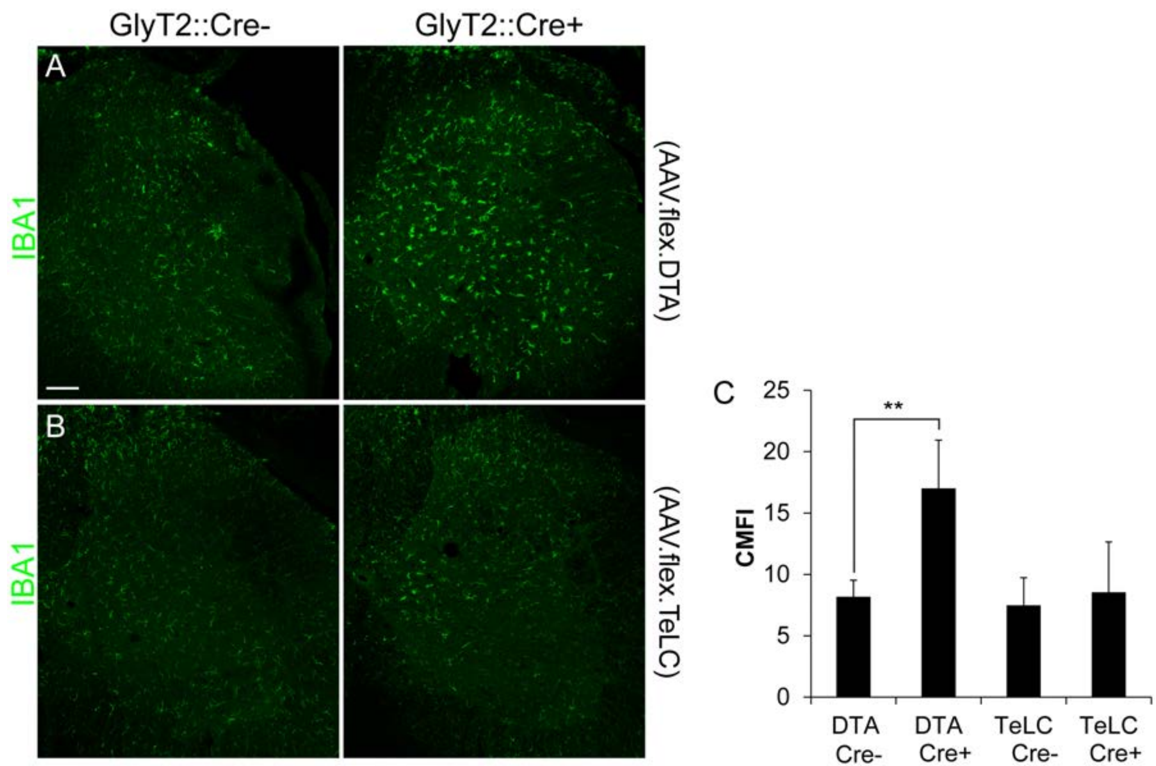

Figure S6 (related to Figure 6). Microglia activation after intraspinal AAV injection
Sections of spinal cords injected with either AAV.flex.DTA (A) or AAV.flex.TeLC (B) were stained with anti-IBA1 (green) antibodies to assess microglia activation. (A) An increased IBA1 immunoreactivity was observed 4 d after AAV.flex.DTA injection into the dorsal horn of GlyT2::Cre+ (Cre) mice compared to GlyT2::Cre- littermates. (B) After AAV.flex.TeLC injection no obvious difference in IBA1 intensity was observed when comparing spinal cord sections from Cre+ or Cre- mice. (C) Quantification of the corrected mean fluorescence intensity (CMFI, mean ± SD) in spinal cord sections after the injection of AAV.flex.DTA (DTA) or AAV.flex.TeLC (TeLC) into GlyT2::Cre+ or GlyT2::Cre- mice. Statistics: **, $P < 0.01$ (unpaired t-test), data are from 4 – 5 mice of both genotypes, and 3 sections per mouse. Scale bar 100 µm.

Supplemental Experimental Procedures

Generation of GlyT2::Cre mice

Cre cDNA followed by the bovine growth hormone polyadenylation (poly-A) signal was placed in frame into the start of exon 2 of the *GlyT2* (*slc6a5*) gene (on BAC clone RP23-365E4) using homologous recombination in bacteria (Copeland et al., 2001) thereby replacing exon 2 of the *GlyT2* gene. Mice derived from BAC DNA-injected C57BL/6 oocytes were screened by PCR for the presence of Cre and for the two BAC ends. Transgenic mice were maintained on a C57BL/6J background.

Immunohistochemistry

Mice were perfused with 4% paraformaldehyde (PFA) in PBS followed by postfixation in 4% PFA in PBS for 1 - 2 hours. The tissue was cut into 25 µm cryosections, which were mounted onto Superfrost Plus microscope slides (Thermo Scientific, Zurich, Switzerland). The following antibodies were used: goat anti-βGal (1:1000, Abcam, Cambridge, UK), goat anti-CGRP (1:500, Abcam, Cambridge, UK), mouse anti-Cre (1:1000, Abcam, Cambridge, UK), rabbit anti-c-fos (1:5000, Millipore, Billerica MA, USA), rabbit anti-GFP (1:1000 or 1:3000; Molecular Probes Inc., Eugene, OR, USA), sheep anti-eGFP (1:1000; AbD Serotec, Kidlington, UK), rabbit anti-IBA1 (1:1000, Wako, Neuss, Germany), rabbit and guinea pig anti-Lmx1b (1:10,000; gift from Dr Carmen Birchmeier, MDC Berlin), Rabbit anti-NF200 (1:2000, Sigma, St. Louis, US), Rabbit anti-NeuN (1:3000, Abcam, Cambridge, UK), goat anti-nNos (1:1000, Abcam, Cambridge, UK), goat anti-Pax2 (1:200, R&D systems, Minneapolis, US), rabbit anti-Pax2 (1:400; Invitrogen, Carlsbad, USA), rabbit anti-PKCγ (1:1000; Santa Cruz, Dallas, TX, USA), rabbit anti-TVA (generous gift from D. Saur; Seidler et al., 2008), rabbit anti-vAChT (1 : 2000; Synaptic Systems, Göttingen, Germany) and cyanine 3 (Cy3)-, Alexa Fluor 488-, DyLight 488-, 647- and 649-conjugated donkey secondary antibodies (Dianova, Hamburg, Germany). To detect IB4+ neurons the isolectin IB4 Alexa Fluor 647 conjugate (Life Technologies, Carlsbad, US) was used.

Image analysis

Fluorescent images were acquired on a Zeiss LSM710 Pascal confocal microscope using a 0.8 NA × 20 Plan-apochromat objective or a 1.3 NA × 40 EC Plan-Neofluar oil-immersion objective and the ZEN2012 software (Carl Zeiss). Whenever applicable, contrast, illumination, and false colors were adjusted in ImageJ or Adobe Photoshop (Adobe Systems, Dublin, Ireland). For cell counts in tissue sections, section were prepared from at least three animals and at least three sections were analyzed per animal. In order to avoid double counting of cells in adjacent sections, all sections used for quantification were taken at a rostro-caudal distance of at least 50 µm. Numbers of immunoreactive cells were determined using the ImageJ Cell Counter plug-in. In order to quantify controlled mean fluorescent intensity (CMTF) in tissue sections the gray matter in a spinal cord section was selected and the measure function of ImageJ was used to determine the mean fluorescent intensity. The CMTF was calculated by subtracting the mean value of four randomly selected background regions from the mean fluorescent value of the grey matter.

AAV preparation

AAV.flex.DTA and AAV.flex.TeLC vectors were cloned in-house and packaged at Penn Vector Core (Perelman School of Medicine, University of Pennsylvania) using their custom service. AAV.flex.DTA and AAV.flex.TeLC vectors were cloned by excising the ChR2-mCherry fusion protein from pAAV-Ef1a-DIO-hChR2(H134R)-mCherry-WPRE-pA (kindly provided by Dr. Karl Deisseroth, Stanford University) with AscI and NheI and replacing it with PCR amplified DTA or TeLC cDNA. DTA cds was amplified from pDTA vector and TeLC cds was amplified from pGEM-EZ-TeTx plasmid (kind gift of Dr Ron Yu, Stowers Institute for Medical Research, Kansas City, MO). AAV 2/1 vectors were used for all experiments described in this study with the exception of AAV.flex.hM3Dq-mCherry, which was serotype 2 (UNC Vector Core, Chapel Hill, NC) and the eGFP expressing reporter vector, which was serotype 9. All three AAVs have previously been shown to efficiently transduce neurons in the CNS (Weinberg et al., 2013).

Intraspinal AVV injections

Animals were anesthetized with 2 - 5% isofluorane and lumbar vertebrae L4 and L5 were exposed. The animal was then placed in a motorized stereotaxic frame and the vertebral column was immobilized

using a pair of spinal adaptors. The vertebral lamina and dorsal spinous process were removed to expose the L4 lumbar segment. The dura was perforated about 500 µm left of the dorsal blood vessel using a beveled 27G needle. Viral vectors were injected at a depth of 200 - 300 µm using a glass micropipette (tip diameter 30 - 40 µm) attached to a 10 µl Hamilton syringe. The rate of injection (30 nl/min) was controlled using a PHD Ultra syringe pump with a nanomite attachment (Harvard Apparatus, Holliston, MA). The micropipette was left in place for 5 min after the injection. Wounds were sutured and the animals were injected i.p. with 0.03 mg/kg buprenorphine and allowed to recover on a heat mat.

Retrograde tracing experiments

For retrograde monosynaptic tracing experiments, we used a two-step strategy that involved injection an AAV helper virus (AAV.flex.TVA.2A.RbG) containing a Cre-dependent TVA (avian tumor virus receptor A) and rabies glycoprotein (RbG) expression cassette and a subsequent injection of an EnvA (avian sarcoma leukosis virus "A" envelop glycoprotein) pseudotyped glycoprotein-deficient rabies virus (EnvA.RabiesΔG.eGFP). The TVA protein expressed from the helper virus enabled cell type-specific infection of GlyT2::Cre+ neurons, and the RbG was expressed to transcomplement the glycoprotein-deficient rabies virus in the primary infected neurons. GlyT2::Cre+ mice received two unilateral injections of AAV.flex.TVA.2A.RbG (2.9 x 10^9 GC per injection in 300 nl) into L3 and L4 segments of the dorsal horn. The vertebral lamina was left intact in order to limit the adhesion of scar tissue to the dorsal surface of the spinal cord. The mice were allowed to recover and then 14 days before they received an injection of EnvA.RabiesΔG.eGFP (1 x 10^6 GC per injection in 500 nl) into the same site. The brain, spinal cord and DRGs were harvested 7 days later.

Electrophysiology and optogenetics

Optogenetic experiments were made in vGAT::ChR2-eYFP;GlyT2::Cre double transgenic mice and in vGAT::ChR2-eYFP control (GlyT2::Cre-) mice of either sex. At P18, mice received two unilateral injections of AAV.flex.DTA together with AAV.mCherry (both 1 x 10^9 vector particles/ injection). Four to 8 days later, mice were decapitated in deep isoflurane anesthesia. Transverse spinal cord slices were prepared as described by (Dugue et al., 2009). During recordings, slices were continuously superfused with aCSF containing (in mM): 120 NaCl, 2.5 KCl, 1.25 NaH_2PO_4, 26 $NaHCO_3$, 5 HEPES, 1 $MgCl_2$, 2 $CaCl_2$ and 14.6 glucose, equilibrated with 95% O_2, 5% CO_2. Whole-cell patch-clamp recordings were made at room temperature from lamina I/II neurons of the infected area, which could easily be identified by its red fluorescence. Recorded neurons were held at -70 mV using an EPC 9 amplifier (HEKA Elektronik, Lambrecht, Germany) controlled with Patchmaster acquisition software. Patch pipettes (resistance 4 - 5 MΩ) were filled with intracellular solution containing (in mM): 120 CsCl, 2 $MgCl_2$ 6 H_2O, 10 HEPES, 0.05 EGTA, 2 MgATP, 0.1 NaGTP, 5 QX-314 (pH 7.35). Light-evoked IPSCs were elicited at a frequency of 5 / min by wide field illumination of the ispilateral dorsal horn (473 ± 5 nm wave length, 2.7 mW, 4 ms) using a Polychrome V monochromator (Till Photonics, Gräfelfing, Germany). Access resistance was monitored with short hyperpolarizing voltage steps (-5 mV) between the synaptic stimulations.

Behavioral analyses

Adult male GlyT2::Cre+ mice (4 – 5 weeks-old) received three unilaterally injections (300 nl) at level L3 – L5 with AAV.flex.DTA (1 x 10^9 virus particles/injection), AAV.flex.TeLC-FLAG (2 x 10^8 virus particles/injection) or AAV.flex.hM3Dq-mCherry (5 x 10^8 particles/injection). Animals injected with AAV.flex.DTA were also co-injected with AAV.eGFP (1 x 10^9 virus particles/injection). Experimenters were blinded to either genotype or treatment, and only mice that did not show obvious (motor) impairments were used.

Mechanical withdrawal thresholds and thermal withdrawal latencies were assessed using an electronic von Frey anesthesiometer and Hargreaves test apparatus with a temperature controlled glass platform (30°C) (both from IITC, Woodland Hills, CA). Responses to noxious cold were determined following the protocol by (Brenner et al., 2012) using a 5 mm thick borosilicate glass platform. Baseline measurements were recorded on two consecutive days prior to surgery. Six measurements were recorded for each animal, and the ipsilateral and contralateral paws were tested alternately. Motor coordination was tested using an accelerating rotarod (IITC,

Woodland Hills, CA). Mice were trained on 2 consecutive days and the maximum number of rotations per minute (rpm) that caused the animal to fall was recorded. The rod was programmed to accelerate from 0 to 40 rpm over 300 s. On experimental days, each mouse was allowed three trials and the average rpm at the point of failure was recorded. Animals were videotaped for 5 min to allow off-line quantification of spontaneous aversive behaviors (flinching and the time spent licking/biting).

Animals injected with AAV.flex.hM3Dq-mCherry (Alexander et al., 2009) were subjected to a chronic constriction injury of the sciatic nerve (Bennett and Xie, 1988) 7 days post virus injection. Baseline mechanical thresholds were recorded before and after surgery. Seven days post surgery, the animals were injected i.p. with 1 mg/kg clozapine *N*-oxide (CNO, Sigma) or vehicle (saline with 0.5% DMSO) and mechanical sensitivity of the ipsilateral and contralateral paws was measured every 15 min for 5 hours, and 24 hours after drug administration.

The horizontal wire test (Bonetti et al., 1982) was used to assess potential muscle relaxation. Mice were placed forepaws-first onto a metal wire and scored according to whether or not they were able to grasp the wire with their hindpaws.

Itch responses were assessed 14 days after intraspinal AAV.flex.hM3Dq-mCherry injection. Mice were treated with either CNO (1 mg/kg, i.p.) or vehicle. The animals were allowed to settle for 60 min before histamine or chloroquine were intracutaneously injected at the plantar surface of the left hind paw (i.e. ipsilateral to the virus injection).

Statistical analyses

Unless otherwise indicated, all data are given as mean ± SEM. Statistical comparisons were made using unpaired or paired t-tests, one-way ANOVA, repeated measures ANOVA, two-way ANOVA or two-way repeated measures ANOVA followed by appropriate *post hoc* tests.

Supplemental References

Alexander, G.M., Rogan, S.C., Abbas, A.I., Armbruster, B.N., Pei, Y., Allen, J.A., Nonneman, R.J., Hartmann, J., Moy, S.S., Nicolelis, M.A.*, et al.* (2009). Remote control of neuronal activity in transgenic mice expressing evolved G protein-coupled receptors. Neuron 63, 27-39.

Bennett, G., and Xie, Y. (1988). A peripheral mononeuropathy in rat that produces disorders of pain sensation like those seen in man. Pain 33, 87-107.

Bonetti, E.P., Pieri, L., Cumin, R., Schaffner, R., Pieri, M., Gamzu, E.R., Muller, R.K., and Haefely, W. (1982). Benzodiazepine antagonist Ro 15-1788: neurological and behavioral effects. Psychopharmacology (Berl) 78, 8-18.

Brenner, D.S., Golden, J.P., and Gereau, R.W.t. (2012). A novel behavioral assay for measuring cold sensation in mice. PLoS One 7, e39765.

Copeland, N.G., Jenkins, N.A., and Court, D.L. (2001). Recombineering: a powerful new tool for mouse functional genomics. Nat Rev Genet 2, 769-779.

Dugue, G.P., Brunel, N., Hakim, V., Schwartz, E., Chat, M., Levesque, M., Courtemanche, R., Lena, C., and Dieudonne, S. (2009). Electrical coupling mediates tunable low-frequency oscillations and resonance in the cerebellar Golgi cell network. Neuron 61, 126-139.

Punnakkal, P., von Schoultz, C., Haenraets, K., Wildner, H., and Zeilhofer, H.U. (2014). Morphological, Biophysical and Synaptic Properties of Glutamatergic Neurons of the Mouse Spinal Dorsal Horn. J Physiol 592, 759-776.

Seidler, B., Schmidt, A., Mayr, U., Nakhai, H., Schmid, R.M., Schneider, G., and Saur, D. (2008). A Cre-loxP-based mouse model for conditional somatic gene expression and knockdown in vivo by using avian retroviral vectors. Proc Natl Acad Sci U S A 105, 10137-10142.

Weinberg, M.S., Samulski, R.J., and McCown, T.J. (2013). Adeno-associated virus (AAV) gene therapy for neurological disease. Neuropharmacology 69, 82-88.